Rev.Adv.Mater.Sci. 19 (2009) 103-113

TRANSITION FROM PLASTIC SHEAR INTO ROTATION DEFORMATION MODE IN NANOCRYSTALLINE METALS AND CERAMICS

S.V. Bobylev[1], A.K. Mukherjee[2] and I.A. Ovid'ko[1]

[1]Institute of Problems of Mechanical Engineering, Russian Academy of Sciences, Bolshoj 61, Vasil. Ostrov, St. Petersburg 199178, Russia
[2]University of California, Davis, 1 Shields Avenue, Davis, CA 95616, USA

Received: November 24, 2008

Abstract. A theoretical model is suggested which describes transition from plastic shear into rotation deformation mode - deformation accompanied by crystal lattice rotations - in nanocrystalline metals and ceramics. Within the model, the shear deformation occurs through either grain boundary sliding or lattice dislocation slip and results in formation of pile-ups of either grain boundary or lattice dislocations, respectively. The dislocation pile-ups create stress fields initiating the rotation deformation (occurring through formation of immobile disclinations whose strengths gradually increase during the formation process) in neighboring nanograins. These processes provide transition from plastic shear into rotation deformation mode in nanocrystalline metals and ceramics, including single-phase nanocrystalline materials with narrow and bimodal grain size distributions as well as nanocomposites consisting of microscale grains and nanoparticles. The conditions are calculated at which the transition is energetically favorable in nanocrystalline Ni and α-Al_2O_3 (corundum).

1. INTRODUCTION

Nanocrystalline metallic and ceramic materials show unique deformation behaviors and outstanding mechanical properties due to the nanoscale and interface effects; see, e.g., [1–12]. In particular, specific plastic deformation mechanisms carried by grain boundaries effectively operate in nanomaterials characterized by large volume fractions occupied by these boundaries and their triple junctions. Such mechanisms include grain boundary sliding, grain boundary diffusional creep (Coble creep) and rotation deformation mode [1–12]. The mechanisms conducted by grain boundaries significantly or even dominantly contribute to plastic flow in nanomaterials. In many cases, these mechanisms operate in parallel with the conventional lattice dislocation slip and effectively compete with it in mechanically loaded nanomaterials [1–12].

Of particular interest is the rotation deformation mode – plastic deformation accompanied by local rotations of crystal lattice within nanoscale grains – in nanomaterials [1,12–40]. For instance, following experimental data [18–28], computer simulations [29–32] and theoretical models [33–38], stress-driven grain boundary migration represents a rotation deformation mechanism effectively operating in nanomaterials. Besides, crystal lattice rotations in nanograins without grain boundary migration were experimentally observed in nanomaterials at plastic and superplastic deformation regimes [1,3–15].

Corresponding author: I.A. Ovid'ko, e-mail: ovidko@def.ipme.ru

Elemental carriers of rotation deformation in nanomaterials are commonly treated to be wedge disclinations – line defects of the rotation type – nucleating at and moving along grain boundaries [17,33,35–38].

The rotation deformation mode often operates in nanomaterials in parallel with the lattice dislocation slip and grain boundary sliding that represent typical plastic shear deformation modes. For instance, it is the case of nanomaterials under superplastic deformation predominantly occurring through the grain boundary sliding and involving both the lattice dislocation slip and the rotation deformation mode [1,12]. In doing so, the rotation and shear deformation mechanisms can operate in neighboring grains and produce strain incompatibilities, if transfer from one deformation mode to another is not effective. In their turn, the strain incompatibilities create high local stresses capable of inducing crack nucleation. In this context, in order to control/avoid formation of dangerous strain incompatibilities, it is important to understand micromechanisms for effective transition between the rotation and shear deformation modes in nanocrystalline materials. In papers [41,42], such transitions were discussed in terms of *mobile* disclinations as carriers of rotation deformation. Recently, a new rotation deformation mode in nanomaterials has been suggested which is associated with evolution of *immobile* disclinations [43]. The main aim of this paper is to suggest a specific micromechanism for the transition from plastic shear deformation into the rotation deformation mode carried by immobile disclinations.

2. GEOMETRIC FEATURES OF SPECIAL TRANSITION FROM PLASTIC SHEAR INTO ROTATION DEFORMATION MODE IN NANOCRYSTALLINE METALS AND CERAMICS

Let us consider geometric features of the specific micromechanism for the transition from plastic shear deformation (grain boundary sliding or lattice dislocation slip) into the rotation deformation mode carried by immobile disclinations in nanocrystalline metals and ceramics. To do so, we start with a discussion of such geometric features in the case of

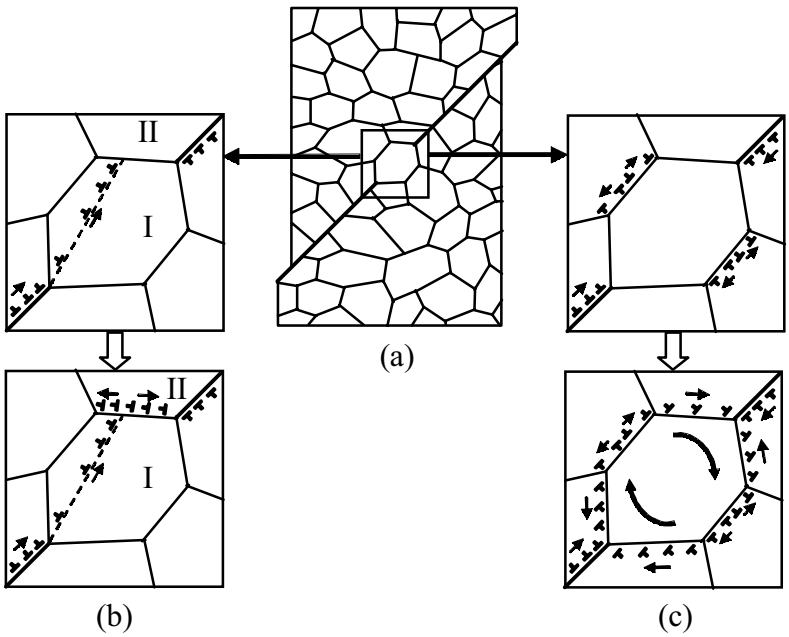

Fig. 1. Shear and rotation deformation modes in a nanocrystalline specimen containing a mesoscopic sliding surface. (a) Enhanced grain boundary sliding along the mesoscopic sliding surface stops at a grain whose geometry prevents such a sliding. Grain boundary dislocations are accumulated at the mesoscopic sliding surface near the grain. (b) Lattice dislocations are emitted from a triple junction into the grain. They transform into grain boundary dislocations whose slow climb controls the rate of both dislocation emission from the triple junction and thereby grain boundary sliding. (c) Shear deformation mode transforms into rotation deformation occurring in the grain. The rotation deformation involves slow climb of grain boundary dislocations, and the climb rate controls the rate of grain boundary sliding.

superplastic deformation of nanocrystalline materials with narrow grain size distributions (Fig. 1a). Following experimental data [44–46], when plastic flow occurs predominantly through grain boundary sliding, it is highly localized in mesoscopic sliding surfaces in nanomaterials at superplastic and high-strain deformation regimes. Each mesoscopic sliding surface represents a chain of several grain boundaries having approximately parallel planes and conducts cooperative grain boundary sliding characterized by very large values of local plastic strain (Fig. 1a) [44–46]. In general, one expects that a mesoscopic sliding surface, at least at the first stage of its formation, consists of several plane fragments divided by grains whose geometry prevents intense grain boundary sliding (Fig. 1a). Further evolution of the system in such grains as well as in other grains whose neighboring grain boundaries conduct grain boundary sliding is conventionally treated to occur through emission of lattice dislocations from triple junctions (Fig. 1b) [47,48]. The lattice dislocations reach a grain boundary (opposite to a triple junction emitting the dislocations) and transform into grain boundary dislocations (Fig. 1b). Then the emitted dislocations create stress fields that suppress both further emission of lattice dislocations from the triple junction and thereby grain boundary sliding [47,48]. However, when the grain boundary dislocations climb far from the triple junction, the junction again becomes active as the lattice dislocation source. In these circumstances, after some time interval, the system will reach its dynamic equilibrium state in which the dislocation emission from the triple junction is completely compensated by the climb of grain boundary dislocations (Fig. 1b). The latter process is slow, because its rate is caused by grain boundary diffusion. As a result, the slow climb of grain boundary dislocations controls comparatively fast processes of both emission of lattice dislocations from triple junctions and thereby grain boundary sliding (for details, see [47,48]).

We think, that besides this conventional evolution scheme (Fig. 1b), the enhanced grain boundary sliding can transform into the slow rotation deformation mediated by diffusion-assisted climb of grain boundary dislocations in these grains (Fig. 1c). For illustration of the defect structure transformation responsible for transition from grain boundary sliding into the rotation deformation, let us consider a model rectangular grain ABCD whose geometry prevents intense grain boundary sliding in a mesoscopic sliding surface in a deformed nanocrystalline specimen (Fig. 2). As a result of the intense grain boundary sliding, two pile-ups of grain boundary dislocations are formed in horizontal fragments EF and GH of the mesoscopic sliding surface in the vicinity of the grain ABCD, as shown in Fig. 2. Within our model, both the external stress and stresses created by the grain boundary dislocation pile-ups initiate special rotation deformation by the immobile disclination mechanism considered in Ref. [43]. More precisely, the formation and evolution of the wedge disclinations at the edges of the rectangular nanograin ABCD is realized by means of grain boundary sliding along horizontal grain boundaries AB and CD as well as grain boundary dislocation climb along vertical grain boundaries AC and BD. In doing so, grain boundary sliding is carried by grain boundary dislocations that are nucleated at grain boundaries AB and CD and slip under the action of the applied shear stress over these GBs (Fig. 2b). In parallel with grain boundary sliding, grain boundary dislocation climb occurs over the vertical grain boundaries AC and BD, in which case the dislocations start to climb from the triple junctions A, B, C, and D (Fig. 2c and 2d). As a result, two grain boundary dislocation walls of opposite signs form at the vertical grain boundaries AC and BD (Figs. 2c and 2d). The formation of these dislocation walls results in plastic deformation of the grain. Also, the grain boundary dislocation walls create stresses and produce extra tilt misorientation of the vertical grain boundaries AC and BD (Figs. 2c and 2d), compared to the initial state (Fig. 2a).

Following the theory of defects in solids [49,50], finite grain boundary dislocation walls, AC and BD, create elastic stresses and local lattice rotations effectively approximated as those created by a quadrupole of wedge disclinations located at the nanograin edges A, B, C, and D (Figs. 2c and 2d). As to more details, according to definition of disclinations in nano- and polycrystalline solids [49,50], a wedge disclination represents a rotation line defect located at either a grain boundary or a triple junction of grain boundaries and characterized by the disclination strength, the rotation misfit (angle gap). For instance, a wedge disclination at a tilt grain boundary is the line dividing grain boundary fragments with different tilt misorientation angles, whose difference is the disclination strength. A wedge disclination exists at a triple junction of tilt boundaries, if the sum of tilt misorientation angles of these boundaries is non-zero [49,50]. The non-zero sum (angle gap) serves as the disclination strength. In particular, it is the case under consideration (Figs. 2c and 2d), because extra tilt misorientation of the

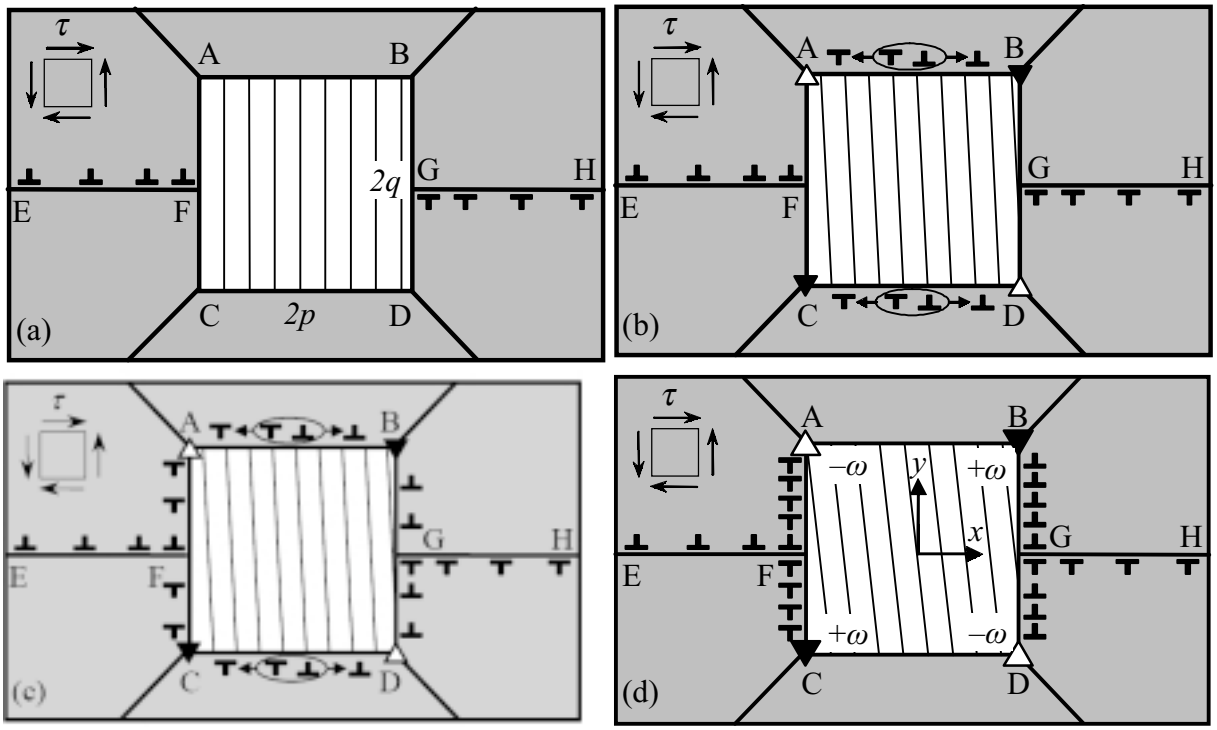

Fig. 2. Model of rotation deformation initiated by grain boundary sliding. (a) Initial structure containing a rectangular grain ABCD. Two pile-ups of grain boundary dislocations are formed at segments EF and GH of mesoscopic sliding surface. (b) New grain boundary dislocations are generated at horizontal grain boundaries AC and BD under the action of the external shear stress and the stress fields of the pile-ups of grain boundary dislocations. (c) and (d) Special rotation deformation occurs in a nanograin through formation of immobile disclinations (triangles) whose strengths gradually increase during the formation process conducted by grain boundary dislocation slip and climb. In the situation (d), the system reaches its dynamic equilibrium state in which the dislocation generation at the horizontal grain boundaries AB and CD as well as within the mesoscopic sliding surface segments EF and GH is completely compensated by the dislocation annihilation at the triple junctions F and G.

vertical grain boundaries AC and BD violates the initial balance of grain boundary misorientations at the triple junctions A. B, C, and D. The strength magnitudes of the disclinations under our consideration (Figs. 2c and 2d) gradually increase with rising the density of grain boundary dislocations at the vertical grain boundaries AC and BD.

The grain boundary dislocations of the pile-up in the segment EF (GH, respectively) of the mesoscopic sliding surface have Burgers vectors with directions opposite to those of Burgers vectors of grain boundary dislocations that climb along the vertical grain boundary AC (BD, respectively) (Fig. 2). As a corollary, when the grain boundary dislocations having opposite Burgers vector directions meet at the triple junctions F and G, they annihilate. In these circumstances, after some time interval, the system reaches its dynamic equilibrium state in which the dislocation generation at the horizontal grain boundaries AB and CD as well as within the mesoscopic sliding surfaces EF and GH is completely compensated by the dislocation annihilation at the triple junctions F and G. The dynamic equilibrium state is characterized by the presence of immobile disclinations having some equilibrium disclination strengths and creating local lattice rotations. In section 3, we will consider the energy and stress characteristics of this dynamic equilibrium state.

Now let us turn to a discussion of the special transition in other situations, different from that shown in Figs. 1c and 2. First, note that the grain-boundary-sliding-induced emission of lattice dislocations from triple junctions (Fig. 1b), in fact, creates a pile-up consisting of both lattice and grain boundary dislocations. The pile-up can induce the rotation deformation in the neighboring grain (grain II in Fig. 1b) in the same way as with the pile-ups of grain boundary dislocations at mesoscopic sliding surfaces (Figs. 1c and 2).

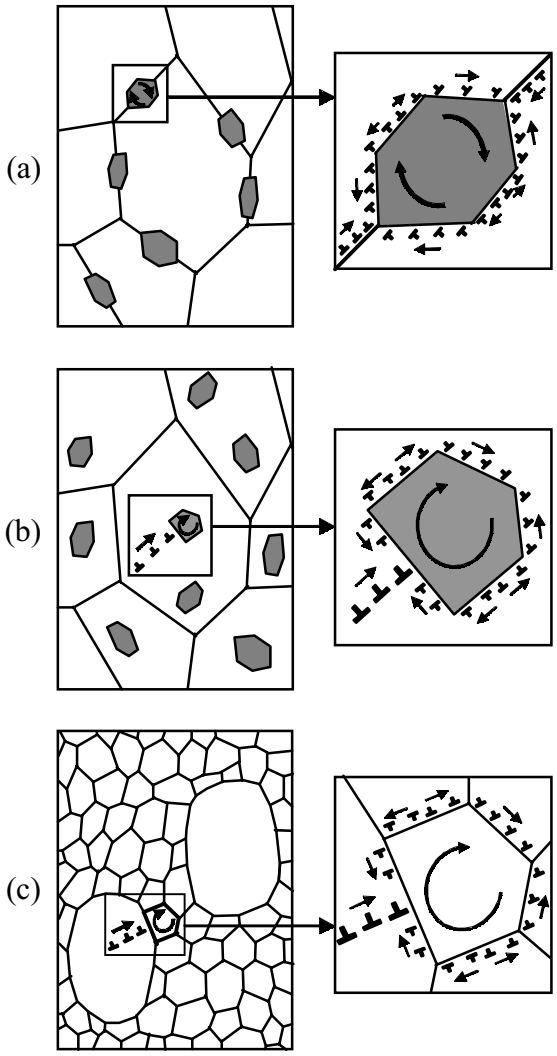

Fig. 3. Transition of plastic shear into rotation deformation mode occurs in (a) ceramic nanocomposite containing nanoparticles at grain boundaries, (b) ceramic nanocomposite containing nanoparticles in grain interiors, and (c) nanomaterial with a bimodal grain size distribution (for details, see text).

Also, the transition from grain boundary sliding into the rotation deformation (Figs. 1c and 2) can occur in ceramic nanocomposites consisting of microscale grains with nanoparticles at either grain boundaries (Fig. 3a) or in grain interiors (Fig. 3b) as well as nanomaterials with a bimodal structure consisting of large grains embedded into a nanocrystalline matrix (Fig. 3c). In the first case, grain boundary sliding commonly occurs along grain boundaries, and nanoparticles serve as obstacles for this process. The grain boundary sliding is hampered at the nanoparticles and can induce the rotation deformation (Fig. 3a).

In the case of nanocomposites consisting of comparatively soft microscale grains with hard nanoparticles in grain interiors (Fig. 3b), plastic flow starts to occur by the lattice dislocation slip in “soft” grain interiors. The nanoparticles serve as obstacles for lattice dislocations that can form pile-ups near the nanoparticles and induce the rotation deformation in them (Fig. 3b).

Plastic flow in nanomaterials with a bimodal structure (Fig. 3c) commonly starts to occur by the lattice dislocation slip in “soft” large grains, while the comparatively “hard” nanocrystalline matrix is not involved into the first stage of plastic deformation [4,11]. In these circumstances, one expects that lattice dislocation pile-ups are formed near grain boundaries serving as obstacles for the lattice dislocation slip (Fig. 3c). The lattice dislocation pile-ups create stresses capable of initiating the rotation deformation in nanoscale grains adjacent to large grains at the second stage of plastic deformation (Fig. 3c). The discussed examples (Figs. 1 and 3) represent typical scenarios for transition from plastic shear deformation (grain boundary sliding or lattice dislocation slip) into the rotation deformation mode carried by immobile disclinations in nanocrystalline metals and ceramics.

3. ENERGY CHARACTERISTICS OF SPECIAL TRANSITION FROM PLASTIC SHEAR INTO ROTATION DEFORMATION MODE IN NANOCRYSTALLINE METALS AND CERAMICS

Let us consider the energy characteristics of the special transition from plastic shear into rotation deformation mode in nanomaterials. To do so, for simplicity, we will examine such characteristics in the two-dimensional model situation with rectangular crystalline grain ABCD dividing two segments EF and GH of a mesoscopic sliding surface in a nanocrystalline specimen (Fig. 2). Two pile-ups of grain boundary dislocations are formed in the segments, EF and GH, perpendicular to the vertical grain boundaries AC and BD, as shown in Fig. 2. Each of the dislocation pile-up at the mesoscopic sliding surface segment EF (GH, respectively) is supposed to consist of n identical edge dislocations with Burgers vectors $\boldsymbol{b}$ ($-\boldsymbol{b}$, respectively). The head dislocations of the pile-ups are located at centers of the vertical grain boundaries AC and BD (Fig. 2). In

accordance with our previous description of the special transition (section 2), it results in the generation of a quadrupole of immobile wedge disclinations at triple junctions A, B, C, and D in the superposition of both the external stress τ and the stress field created by the dislocation pile-ups (Fig. 2). The disclination quadrupole is characterized by sizes $2p \times 2q$ and disclination strengths $\pm\omega$. Within our model, the nanocrystalline specimen containing the disclination quadrupole is assumed to be an elastically isotropic solid having the shear modulus G and the Poisson ratio ν. The model (Fig. 2) is simple enough for its effective theoretical analysis and, at the same time, captures the essential micromechanics of the special transition from plastic shear into rotation deformation mode in nanomaterials.

Let us calculate the energy change ΔW due to the generation of a disclination quadrupole in the framework of the model (Fig. 2) under consideration. The energy change has the three terms:

$$\Delta W = W_{el}^{q} + 2W_{\text{int}}^{q-d} - A, \qquad (1)$$

Here W_{el}^{q} is the proper energy of the disclination quadrupole; A denotes the work of the external stress τ, which is spent to the generation of the disclination quadrupole; and W_{int}^{q-d} is the energy that characterizes the interaction between the disclination quadrupole and one of the dislocation pile-ups. With symmetry of the model (Fig. 2) taken into account, the interaction of the disclination quadrupole with the dislocation pile-up at the mesoscopic sliding surface segment EF is identical to that with the dislocation pile-up at the mesoscopic sliding surface segment GH. Therefore, W_{int}^{q-d} is multiplied by factor 2 on the right-hand side of formula (1).

In the discussed model geometry, following Ref. [33], the energy W_{el}^{q} is written as follows:

$$W_{el}^{q} = 2D\omega^2 q^2 \left[(1+t^2)\ln(1+t^2) - t^2 \ln t^2 \right], \qquad (2)$$

where $t=p/q$, $D=G/[2\pi(1-\nu)]$. Also, following Ref. [33], the work A is given as:

$$A = 4\tau\omega pq. \qquad (3)$$

Let $W_{\text{int}}^{q-d}(x_i)$ be the energy that characterizes the interaction of the disclination quadrupole with the ith dislocation belonging to a pile-up and having the coordinate x_i (i = 1,...,n) in the coordinate system associated with the disclination quadrupole center, as shown in Fig. 2d. (In this coordinate system, both the dislocation pile-ups are located in the plane y=0.) The sum interaction energy W_{int}^{q-d} figuring on the right-hand side of formula (1) represents the sum of the energies over index i ranging from 1 to n. The energy can be calculated in the standard way [51] as the work spent to the generation of the i-th dislocation in the stress field created by the disclination quadrupole. In doing so, with known expressions for the stress fields of the disclinations [49], we find:

$$W_{\text{int}}^{q-d}(x_i) = D\omega bq \ln \frac{(x_i - p)^2 + q^2}{(x_i + p)^2 + q^2}. \qquad (4)$$

Then, the sum interaction energy W_{int}^{q-d} is written as:

$$W_{\text{int}}^{q-d} = D\omega bq \sum_{i=1}^{n} \ln \frac{(x_i - p)^2 + q^2}{(x_i + p)^2 + q^2}, \qquad (5)$$

Following the method [51], the coordinates x_i of the dislocations belonging to the pile-up are calculated as roots of the first derivatives of the corresponding Laguerre polynoms. With formulas (2), (3) and (5) substituted to the expression (1), after some algebra, we find the energy change ΔW as follows:

$$\Delta W = 2D \left\{ \omega^2 q^2 \left[(1+t^2)\ln(1+t^2) - t^2 \ln t^2 \right] + \omega qb \sum_{i=1}^{n} \ln \frac{(x_i - qt)^2 + q^2}{(x_i + qt)^2 + q^2} - 2(\tau / D)\omega q^2 t \right\}. \qquad (6)$$

The dependences ΔW (in units of $2Db^2$) on ω are presented in Fig. 4, for various values of the external shear stress (τ/D) and parameter $t=p/q$ at n=5 and q=100b. For q~10nm and typical value of the Burgers vector magnitude $b \approx$ 0.1nm of grain boundary dislocations, the length of the dislocation pile-up is ~100b≈10nm at given values of the parameters of the system.

Strictly speaking, though the expression (6) might be written in normalized parameters ($\Delta W/(2Db^2)$, τ/D, x_i/b, q/b), it is not universal for all materials. It is because the dislocation coordinates x_i depend on material parameters. Nevertheless, our calculations have shown that sensitivity of x_i on material parameters is weak, since the crucial contribution to the total interaction energy W_{int}^{q-d} is given by the head dislocations of the pile-up, and the coordinates of the head dislocations weakly depend on material parameters. In this context, despite the fact that the dependences shown in Fig. 4 are calculated in the case of Ni (with G=73 GPa, ν=0.34 [53]), these dependences are, by practice, universal. In particu-

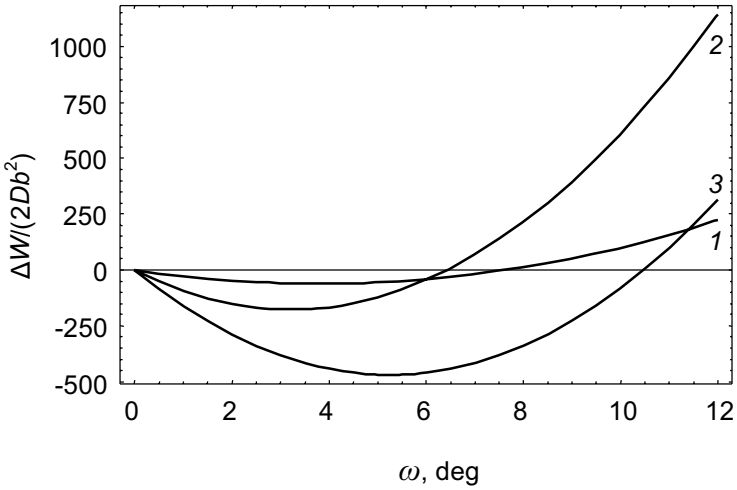

Fig. 4. Dependences of ΔW (in units of $2Db^2$) on disclination strength ω, for various values of the external shear stress (τ/D) and parameter $t=p/q$ at n=5 and q=100b. Curves *1*, *2,* and *3* correspond to values of τ/D = 0.01, 0.03, and 0.05, respectively.

lar, for nanocrystalline ceramic α-Al_2O_3 with elastic constants (G=169 GPa, ν=0.23 [53]) significantly differing from those of Ni, the dependences in question are very close to those shown in Fig. 4.

According to Fig. 4, the energy ΔW has its minimum at some equilibrium value of the disclination strength ω_0. The equilibrium value is derived from the condition $(\partial\Delta W/\partial\omega)\big|_{\omega=\omega_0}=0$ as follows:

$$\omega_0 = \frac{2(\tau/D)qt - b\sum_{i=1}^{n}\ln\frac{(x_i-p)^2+q^2}{(x_i+p)^2+q^2}}{2q[(1+t^2)\ln(1+t^2)-t^2\ln t^2]}. \qquad (7)$$

The dependences of ω_0 on parameter p/q are presented as solid curves in Fig. 5, for n=5, q=100b and various levels of the external stress. For com-

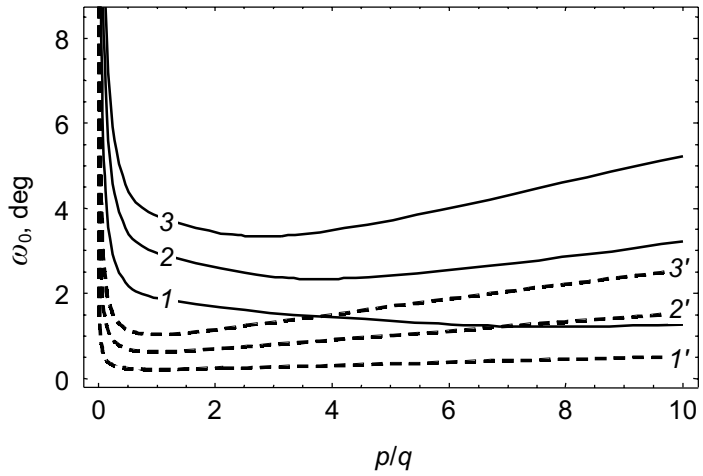

Fig. 5. Dependences of the equilibrium disclination strength ω_0 on parameter p/q are shown as solid curves in the presence of the dislocation pile-ups, for n=5, q=100b and various levels of the external stress. Solid curves *1*, *2,* and *3* correspond to values of τ/D=0.01, 0.03 and 0.05, respectively. For comparison, dashed curves are presented which show the dependences of the equilibrium value ω_0 on parameter p/q in the situation where the dislocation pile-ups are absent. Dashed curves *1'*, *2'* and *3'* correspond to values of 0.03 and 0.05, respectively.

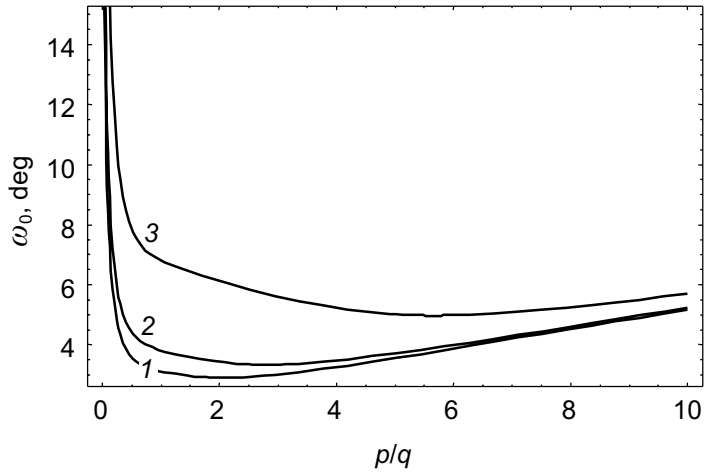

Fig. 6. Dependences of the equilibrium disclination strength ω_0 on parameter *p/q*, are shown as solid curves in the presence of the dislocation pile-ups, for τ/D=0.05, *q*=100*b* and various values of *n*. Curves *1*, *2,* and *3* correspond to values of *n*=3, 5, 7, respectively.

parison, dashed curves are presented in Fig. 5 which show the dependences of the equilibrium value on parameter *p*/*q* in the earlier examined [43] situation where the dislocation pile-ups are absent. (In this situation, *b*=0 in formula (7)). As it follows from Fig. 5, the equilibrium value ω_0 increases by several times due to the presence of the dislocation pile-ups. Besides, dashed curves have their minimums at *p/b*=1 [43], while minimums of the dependences $\omega_0(p/q)$ correspond to larger values of *p/q* in the situation where the dislocation pile-ups exist. In the case of Ni, for *n*=5, *q*=100*b* and the typical stress level τ=0.5GPa, formula (7) gives $\omega_0 \approx 0.050 \approx 2.9^o$ at *p/q*=1, $\omega_0 \approx 0.131 \approx 7.5^o$ at *p/q*=0.1, and $\omega_0 \approx 0.053 \approx 3^o$ at *p/q*=10. In the case of α-Al_2O_3 , for , *n*=5, *q*=100*b* and the typical stress level τ =2 GPa, formula (7) gives: $\omega_0 \approx 0.072 \approx 4.1^o$ at *p/q*=1, $\omega_0 \approx 0.187 \approx 6^o$ at *p/q*=0.1, and $\omega_0 \approx 0.104 \approx 6^o$ at *p/q*=10.

The sensitivity of the equilibrium value ω_0 on the number *n* of dislocations composing a pile-up is illustrated in Fig. 6 where curves *1*, *2,* and *3* correspond to *n*=3, 5, and 10, respectively. In these calculations, other parameters are taken as follows: τ/D=0.05, *q*=100*b*. As it follows from Fig. 6, ω_0 increases with rising *n*.

4. DISCUSSION. CONCLUDING REMARKS

Thus, in this paper, we suggested a theoretical model describing the special micromechanism for transition from plastic shear into rotation deformation mode in such nanomaterials as single-phase nanocrystalline materials with narrow and bimodal grain size distributions as well as nanocomposites consisting of microscale grains and nanoparticles. The plastic shear in these materials occurs through either grain boundary sliding or lattice dislocation slip. Some structural elements serve as obstacles for the plastic shear, in which case pile-ups of either grain boundary or lattice dislocations are formed near these structural elements. For instance, pile-ups of grain boundary dislocations in mesoscopic sliding surfaces are formed near grains that prevent grain boundary sliding and separate various segments of mesoscopic sliding surfaces (Figs. 1c and 2). The dislocation pile-ups create stress fields initiating the rotation deformation in the grains in question (Figs. 1c and 2). The rotation deformation occurs through slip and climb of grain boundary dislocations at grain boundaries of such grains and results in local rotations of their crystal lattices. These processes in a grain are effectively described as formation of immobile disclinations located at triple junctions of grain boundaries of the grain and characterized by disclination strengths gradually increasing during the formation process (Figs. 1c and 2). After some time interval, the system reaches its dynamic equilibrium state characterized by the presence of immobile disclinations having some equilibrium disclination strengths and creating local lattice rotations. Our calculations (section 3) have shown that the special transition from plastic shear into rota-

tion deformation mode is energetically favorable in nanocrystalline Ni and α-Al_2O_3. In doing so, typical values of the equilibrium disclination strength ω_0 range from around 3° to 7.5° in nanocrystalline Ni at the stress level τ=0.5 GPa, and from around 4° to 11° in nanocrystalline α-Al_2O_3 at the stress level τ=2 GPa.

The special transition (Figs. 1c and 2) from grain boundary sliding to the rotation deformation in nanocrystalline materials represents a mechanism for accommodation of grain boundary sliding, which is alternative to the conventional accommodation (Fig. 1b) through emission of lattice dislocations from triple junctions, their transformations into grain boundary dislocations and climb of grain boundary dislocations. The rate of the special transition process is controlled by comparatively slow climb of grain boundary dislocations, whose rate, in its turn, is controlled by grain boundary diffusion. As a corollary, the rate of the special transition (Figs. 1c and 2) is identical to the rate of the conventional accommodation (Fig. 1b) which, following Refs. [47,48], is controlled by the rate of grain boundary diffusion providing climb of grain boundary dislocations. In this context, the rate of grain boundary sliding controlled by the special transition process can be described by the following rate equation [48,54] of the grain boundary sliding accommodated by the conventional mechanism in nanocrystalline materials:

$$\frac{d\varepsilon_{gbs}}{dt} = \frac{AD_{gb}Gb}{kT}\left(\frac{b}{d}\right)^2\left(\frac{\sigma}{G}\right)^2. \qquad (8)$$

Here $d\varepsilon_{gbs}/dt$ denotes the rate of plastic strain carried by grain boundary sliding, t time, A is a dimensionless constant (≈10), D_{gb} the coefficient of grain boundary diffusion, b the dislocation Burgers vector magnitude, σ the stress, d the grain size, k the Boltzmann constant, and T the absolute temperature.

Also, as it was noted in section 2, the grain boundary sliding accommodated by emission of lattice dislocations from triple junctions (Fig. 1b), in fact, creates a pile-up consisting of both lattice and grain boundary dislocations. The pile-up can induce the rotation deformation in the neighboring grain (grain II in Fig. 1b) in the same way as with the pile-ups of grain boundary dislocations at mesoscopic sliding surfaces (Figs. 1c and 2).

Also, the special transition from grain boundary sliding into the rotation deformation can occur in ceramic nanocomposites consisting of microscale grains with nanoparticles (Figs. 3a and 3b) and nanomaterials with bimodal grain size distributions (Fig. 3c). In the case of nanocomposites consisting of microscale grains with nanoparticles at grain boundaries (Fig. 3a), grain boundary sliding commonly occurs along grain boundaries. The nanoparticles serve as obstacles for this process, and pile-ups of grain boundary are formed near them. Such pile-ups can induce the rotation deformation (Fig. 3a). In the case of nanocomposites consisting of comparatively soft microscale grains with hard nanoparticles in grain interiors (Fig. 3b), plastic flow starts to occur by the lattice dislocation slip in "soft" grain interiors. The nanoparticles serve as obstacles for lattice dislocations that can form pile-ups near the nanoparticles and induce the rotation deformation in them (Fig. 3b). Plastic flow in nanomaterials with bimodal grain size distributions (Fig. 3c) commonly starts to occur by the lattice dislocation slip in "soft" large grains, while the comparatively "hard" nanocrystalline matrix in not involved into the first stage of plastic deformation. In these circumstances, one expects that lattice dislocation pile-ups are formed near grain boundaries serving as obstacles for the lattice dislocation slip (Fig. 3c). Then the lattice dislocation pile-ups create stresses capable of initiating the rotation deformation in nanoscale grains adjacent to large grains (Fig. 3c). In the light of the discussed examples (Figs. 1, 2, and 3), the transition from plastic shear deformation (grain boundary sliding or lattice dislocation slip) into the rotation deformation mode carried by immobile

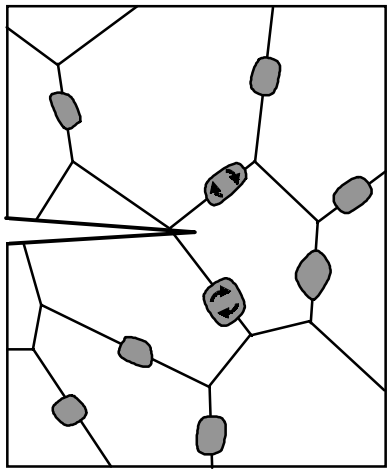

Fig. 7. Rotation deformation (caused by preceding grain boundary sliding and/or lattice dislocation slip) in nanoparticles leads to partial relaxation of high stresses near a crack tip and thereby enhances fracture toughness of a ceramic nanocomposite.

disclinations can be a typical process in single-phase nanocrystalline materials and nanocomposites under plastic deformation. Further experimental examination of the special transition is needed to identify its role in deformation behaviors of nanocrystalline metals and ceramics.

Finally, note that the rotation deformation is enhanced by high stresses in nanomaterials. Therefore, the rotation deformation (caused by preceding grain boundary sliding and/or lattice dislocation slip) is enhanced near a growing crack tip (Fig. 7) where local shear stresses are very high. The rotation deformation is accompanied by formation of wedge disclination quadrupoles whose stresses, according to Ref. [35], compensate for in part the stresses concentrated near the crack tip. As a corollary, the rotation deformation leads to partial relaxation of stresses near a crack tip and thereby is expected to enhance fracture toughness of ceramic nanocomposites.

ACKNOWLEDGEMENTS

The work was supported, in part, by the Russian Federal Agency of Science and Innovations (Contract 02.513.11.3190 of the Program "Industry of Nanosystems and Materials" and grant NSh-2405.2008.1), the National Science Foundation (grants CMMI-0700272 and DMR-0703994), the Russian Foundation of Basic Research (grant 08-01-00225-a), and Russian Academy of Sciences Program "Structural Mechanics of Materials and Construction Elements"

References

[1] A.K. Mukherjee // *Mater. Sci. Eng. A* **322** (2002) 1.
[2] K.S. Kumar, S. Suresh and H. Swygenhoven // *Acta Mater.* **51** (2003) 5743.
[3] S.C. Tjong and H. Chen // *Mater. Sci. Eng. R* **45** (2004) 1.
[4] B.Q. Han, E. Lavernia and F.A. Mohamed // *Rev. Adv. Mater. Sci.* **9** (2005) 1.
[5] I.A. Ovid'ko // *Int. Mater. Rev.* **50** (2005) 65.
[6] D. Wolf, V. Yamakov, S.R. Phillpot, A.K. Mukherjee and H. Gleiter // *Acta Mater.* **53** (2005) 1.
[7] F. Ebrahimi, A.J. Liscano, D. Kong, Q. Zhai and H. Li // *Rev. Adv. Mater. Sci.* **13** (2006) 33.
[8] M.A. Meyers, A. Mishra and D.J. Benson // *Progr. Mater. Sci.* **51** (2006) 427.
[9] M. Dao, L. Lu, R.J. Asaro, J.Th.M. De Hosson and E. Ma // *Acta Mater.* **55** (2007) 4041.
[10] C.C. Koch // *J. Mater. Sci.* **42** (2007) 1403.
[11] I.A. Ovid'ko and A.G. Sheinerman // *Rev. Adv. Mater. Sci.* **16** (2007) 1.
[12] C.C. Koch, I.A. Ovid'ko, S.Seal and S. Veprek, *Structural Nanocrystalline Materials: Fundamentals and Applications* (Cambridge University Press, Cambridge, 2007).
[13] M. Ke, W.W. Milligan, S.A. Hackney, J.E. Carsley and E.C. Aifantis // *Nanostruct. Mater.* **5** (1995) 689.
[14] Zh. Shan, E.A. Stach, J.M.K. Wiezorek, J.A. Knapp, D.M. Follstaedt and S.X. Mao // *Science* **305** (2004) 654.
[15] M. Murayama, J.M. Howe, H. Hidaka and S. Takaki // *Science* **295** (2002) 2433.
[16] I.A. Ovid'ko // *Science* **295** (2002) 2386.
[17] M.Yu. Gutkin and I.A. Ovid'ko, *Plastic Deformation in Nanocrystalline Materials* (Springer, Berlin, 2004).
[18] M. Jin, A.M. Minor, E.A. Stach and J.W. Morris Jr. // *Acta Mater.* **52** (2004) 5381.
[19] W.A. Soer, J.Th.M. De Hosson, A.M. Minor, J.W. Morris Jr. and E.A. Stach // *Acta Mater.* **52** (2004) 5783.
[20] J.T.M. De Hosson, W.A. Soer, A.M. Minor, Z. Shan, E.A. Stach, S.A. Syed Asif and O.L. Warren // *J. Mater. Sci.* **41** (2006) 7704.
[21] K. Zhang, J.R. Weertman and J.A. Eastman // *Appl. Phys. Lett.* **85** (2004) 5197; K. Zhang, J.R. Weertman and J.A. Eastman // *Appl. Phys. Lett.* **87** (2005) 061921.
[22] P.L. Gai, K. Zhang and J.R. Weertman // *Scripta Mater.* **56** (2007) 25.
[23] X.Z. Liao, A.R. Kilmametov, R.Z. Valiev, H. Gao, X. Li, A.K. Mukherjee, J.F. Bingert and Y.T. Zhu // *Appl. Phys. Lett.* **88** (2006) 021909.
[24] D. Pan, T.G. Nieh and M.W. Chen // *Appl. Phys. Lett.* **88** (2006) 161922.
[25] D. Pan, S. Kuwano, T. Fujita and M.W. Chen // *Nano Letters* **7** (2007) 2108.
[26] D.S. Gianola, S. Van Petegem, M. Legros, S. Brandstetter, H. Van Swygenhoven and K.J. Hemker // *Acta Mater.* **54** (2006) 2253.
[27] D.S. Gianola, D.H. Warner, J.F. Molinari and K.J. Hemker // *Scripta Mater.* **55** (2006) 649.
[28] G.J. Fan, L.F. Fu, H. Choo, P.K. Liaw and N.D. Browning // *Acta Mater.* **54** (2006) 4781.
[29] D. Farkas, A. Froseth and H. Van Swygenhoven // *Scripta Mater.* **55** (2006) 695.
[30] J. Monk and D. Farkas // *Phys. Rev. B* **75** (2007) 045414.

[31] F. Sansoz and V. Dupont // *Appl. Phys. Lett.* **89** (2006) 111901.
[32] T. Shimokawa, A. Nakatani and H. Kitagawa // *Phys. Rev. B* **71** (2005) 224110.
[33] M.Yu. Gutkin and I.A. Ovid'ko // *Appl. Phys. Lett.* **87** (2005) 251916.
[34] J.C.M. Li // *Phys. Rev. Lett.* **96** (2006) 215506.
[35] I.A. Ovid'ko, A.G. Sheinerman and E.C. Aifantis // *Acta Mater.* **56** (2008) 2718.
[36] M.Yu Gutkin, K.N. Mikaelyan and I.A. Ovid'ko // *Scripta Mater.* **58** (2008) 850.
[37] I.A. Ovid'ko, A.G. Sheinerman and N.V. Skiba // *Rev. Adv. Mater. Sci.* **16** (2007) 102.
[38] S.V. Bobylev and I.A. Ovid'ko // *Appl. Phys. Lett.* **92** (2008) 081914.
[39] S.P. Joshi and K.T. Ramesh // *Phys. Rev. Lett.* **101** (2008) 025501.
[40] S.P. Joshi and K.T. Ramesh // *Acta Mat*. **56** (2008) 282.
[41] M.Yu. Gutkin, I.A. Ovid'ko and N.V. Skiba // *Acta Mater.* **51** (2003) 4059.
[42] A.L. Kolesnikova, I.A. Ovid'ko and A.E. Romanov // *Tech. Phys. Lett.* **33** (2007) 641.
[43] I.A. Ovid'ko and A.G. Sheinerman // *Scripta Mater.* **59** (2008) 119.
[44] J. Markmann, P. Bunzel, H. Roesner, K.W. Liu, K.A. Padmanabhan, R. Birringer, H. Gleiter, and J. Weissmueller // *Scripta Mater.* **49** (2003) 637.
[45] A.V. Sergueeva and A.K. Mukherjee // *Rev. Adv. Mater. Sci.* **13** (2006) 1.
[46] A.V. Sergueeva, N.A. Mara, N.A. Krasilnikov, R.Z. Valiev and A.K. Mukherjee // *Philos. Mag.* **86** (2006) 5797.
[47] O.A. Ruano, J. Wadsworth and O.D. Sherby // *Acta Mater.* **51** (2003) 3617.
[48] T.G. Langdon // *J. Mater. Sci.* **41** (2006) 597.
[49] A.E. Romanov and V.I. Vladimirov, In: *Dislocations in Solids*, ed. by F.R.N. Nabarro (North Holland, Amsterdam, 1992), Vol. 9, p.191.
[50] M. Kleman and J. Friedel // *Rev. Mod. Phys.* **80** (2008) 61.
[51] J.D. Eshelby, F.C. Frank and F.R.N. Nabarro // Philos. Mag **42** (1951) 351.
[52] C.J. Smithells and E.A. Brands, *Metals Reference Book* (Butterworth, London, 1976).
[53] R.G. Munro // *J. Am. Ceram. Soc.* **80** (1997) 1919.
[54] A.K. Mukherjee, J.E. Bird and J.E. Dorn // *Trans. ASM* **62** (1969) 155.